Layered Imidonitridophosphates

$MH_4P_6N_12$ (M = Mg, Ca): New Imidonitridophosphates with an Unprecedented Layered Network Structure Type

Alexey Marchuk,[a] Vinicius R. Celinski,[b] Jörn Schmedt auf der Günne,*[b] and Wolfgang Schnick*[a]

Abstract: Isotypic imidonitridophosphates $MH_4P_6N_{12}$ (M = Mg, Ca) have been synthesized by high-pressure/high-temperature reactions at 8 GPa and 1000 °C starting from stoichiometric amounts of the respective alkaline-earth metal nitrides, P_3N_5, and amorphous HPN_2. Both compounds form colorless transparent platelet crystals. The crystal structures have been solved and refined from single-crystal X-ray diffraction data. Rietveld refinement confirmed the accuracy of the structure determination. In order to quantify the amounts of H atoms in the respective compounds, quantitative solid-state ^{1}H NMR measurements were carried out. EDX spectroscopy confirmed the chemical compositions. FTIR spectra confirmed the presence of NH groups in both structures. The crystal structures reveal an unprecedented layered tetrahedral arrangement, built up from all-side vertex-sharing PN_4 tetrahedra with condensed *dreier* and *sechser* rings. The resulting layers are separated by metal atoms.

Introduction

Nitridophosphates represent a silicate-analogous class of compounds since the element combination P/N is isoelectronic with Si/O. Consequently, the structural variety of this compound class is expected to be similar to that of silicates. Nitridophosphates can also form anionic tetrahedral network structures made up of condensed PN_4 tetrahedra. Analogously to nitridosilicates, both corner-sharing and edge-sharing PN_4 tetrahedra can occur.[1] Moreover, whereas oxosilicates can only form terminal or singly bridging O^{2-} ions, N atoms in the tetrahedral network structures of nitridophosphates can hypothetically connect up to four tetrahedral centers, as in the nitridosilicates $MYbSi_4N_7$ (M = Sr, Ba).[2] This feature opens up a wide range of new possible crystal structures in the nitridophosphate class of compounds, as well as higher degrees of condensation. With the successful synthesis of the nitridic clathrate $P_4N_4(NH)_4(NH_3)$, we were able to show that the structural diversity of nitridophosphates can even surpass that of oxosilicates.[3] The network structure of this clathrate had been predicted for silica, but has hitherto only been observed in this nitridic compound. The structure of the high-pressure polymorph of silica-analogous phosphorus oxonitride PON has also been predicted for SiO_2, but has yet to be observed as a silica polymorph.[4] The first nitridic zeolites NPO and NPT are further unique representatives in this system.[5–7]

The structural diversity of nitridophosphates is combined with their interesting properties. As an example, phosphorus(V) nitride P_3N_5, which is the binary parent compound of nitridophosphates, can be mentioned. It is used industrially as a flame retardant, as a "getter" material for the elimination of oxygen during the production of incandescent and tungsten halogen lamps, and as a gate insulator material in metal insulator semiconductor field-effect transistors (MISFETs).[8–10] Vitreous compounds in the system Li-Ca-P-N exhibit remarkable refractive indices and hardness values.[11,12] Pseudo-binary phosphorus nitrides PON and HPN_2 are mainly used in the field of flame retardation.[13,14] The nitridic clathrate $P_4N_4(NH)_4(NH_3)$ has been discussed as a possible gas storage or membrane reactor material, due to the encapsulated ammonia within its 4^28^4 cages and its high thermal and chemical stability.[15] Furthermore, $LiPN_2$ and Li_7PN_4 should be mentioned, which exhibit lithium ion conductivity.[16]

Considering all of the aspects mentioned above, it is apparent that the remarkable structural variety of nitridophosphates as well as the resulting diversity of their interesting properties makes a systematic search for new compounds of this type an important research target.

In this contribution, we report on the high-pressure/high-temperature synthesis and structure elucidation of new isotypic imidonitridophosphates $MH_4P_6N_{12}$ (M = Mg, Ca), with an unprecedented layered structure type built up from all-side vertex-sharing PN_4 tetrahedra. In contrast to common nitridophosphates, singly-bridging imide groups NH occur in the network structure. In our preceding publications, we have report-

[a] A. Marchuk, Prof. Dr. W. Schnick
Department Chemie, Ludwig-Maximilians-Universität
Butenandtstrasse 5-13, 81377 München (Germany)
Fax: (+49) 89-2180-77440
E-mail: wolfgang.schnick@uni-muenchen.de

[b] V. R. Celinski, Prof. Dr. J. Schmedt auf der Günne
Inorganic Materials Chemistry, University of Siegen
Adolf-Reichwein-Strasse 2, 57076 Siegen (Germany)
Fax: (+49) 271-740-2555
E-mail: schmedt_auf_der_guenne@chemie.uni-siegen.de

Supporting information for this article is available on the WWW under http://dx.doi.org/10.1002/chem.201406240.

ed on several pseudo-binary phosphorus imide nitrides. Besides α-HPN_2 and its high-pressure polymorph β-HPN_2,[17,18] phosphorus imide nitride α-HP_4N_7 as well as its high-pressure polymorphs β-HP_4N_7 and γ-HP_4N_7 have been described.[19–21] The latter polymorph is the first example of trigonal-bipyramidal coordinated phosphorus being observed in an inorganic network structure. Furthermore, two important representatives of the imidonitridophosphate class of compounds, namely $Na_{10}[P_4(NH)_6N_4](NH_2)_6(NH_3)_{0.5}$ and $Rb_8[P_4N_6(NH)_4](NH_2)_2$, have been mentioned in the literature, both consisting of adamantane-like molecular anions $[P_4N_6(NH)_4]^{6-}$.[22,23] However, to the best of our knowledge no layered (imido)nitridophosphates have hitherto been discussed in the literature.

Results and Discussion

Synthesis

$MH_4P_6N_{12}$ (M = Mg, Ca) were synthesized by high-pressure/high-temperature reaction at 8 GPa and 1000 °C using a Walker-type multi-anvil assembly.[24] Stoichiometric amounts of the respective alkaline-earth metal nitrides, amorphous HPN_2, and P_3N_5 were used as starting materials (Eq. (1)). The products were obtained as air- and moisture-stable colorless crystalline solids. In order to grow single crystals of the respective products, catalytic amounts of NH_4Cl as a mineralizer were added to the starting mixtures. In this way, colorless transparent platelet single crystals of $MH_4P_6N_{12}$ (M = Mg, Ca) were obtained and isolated (Figure 1). As mentioned in a preceding publication, intermediately formed HCl presumably enables reversible cleavage and reformation of P–N bonds and thus facilitates the growth of single crystals.[18] NH_4Cl was removed from the product by washing with de-ionized water and ethanol. Detailed information on the synthesis of the title compounds is given in the Experimental Section.

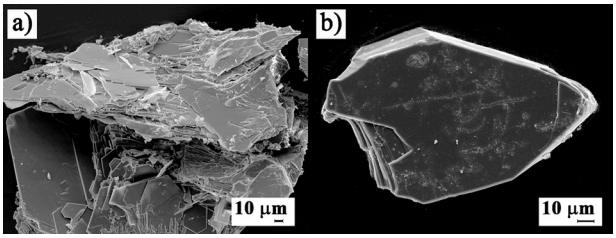

Figure 1. SEM images of crystals of $MH_4P_6N_{12}$, M = Ca (a), Mg (b).

$$M_3N_2 + 12HPN_2 + 2P_3N_5 \rightarrow 3MH_4P_6N_{12} M = \text{Mg, Ca} \quad (1)$$

Structure determination

The crystal structures of $MH_4P_6N_{12}$ (M = Mg, Ca) were solved and refined in the orthorhombic space group *Cmca* (no. 63) from single-crystal X-ray diffraction data using direct methods. For single-crystal structure refinement, the respective lattice parameters from Rietveld refinement were used. The H atom positions were unequivocally determined from difference Fourier syntheses and were refined isotropically using restraints for N-H distances. All non-hydrogen atoms were refined anisotropically. The crystallographic data for $MH_4P_6N_{12}$ are summarized in Table 1; the atomic parameters are given in Tables 2 and 3.

Rietveld refinement based on powder X-ray data corroborated the accuracy of the structure determination of $MH_4P_6N_{12}$

Table 1. Crystallographic data of the single-crystal refinement of $MH_4P_6N_{12}$ (M = Mg, Ca).

Formula	$MgH_4P_6N_{12}$	$CaH_4P_6N_{12}$
Crystal system	orthorhombic	
Space group	*Cmca* (no. 63)	
Lattice parameters [Å][a]	a = 8.4568(16)	a = 8.6289(17)
	b = 4.8270(10)	b = 4.9010(10)
	c = 21.309(4)	c = 22.153(4)
Cell volume [Å^3]	869.8(3)	936.9(3)
Formula units per unit cell	4	4
Density [g·cm^{-3}]	2.919	2.822
μ [mm^{-1}]	1.316	1.703
Radiation	$Mo_{K\alpha}$ (λ = 0.71073 Å)	
Temperature [K]	293(2)	
F(000)	760.0	792.0
Θ range	$3.68° \leq \Theta \leq 27.48°$	$3.82° \leq \Theta \leq 29.99°$
Total no. of reflections	4176	3376
Independent reflections	671 [R(int) = 0.0344]	576 [R(int) = 0.0558]
Refined parameters	54	54
Goodness of fit	1.152	1.119
R_1 (all data); R_1 ($F^2 > 2\sigma(F^2)$)	0.0284; 0.0323	0.0354; 0.0397
wR_2 (all data); wR_2 ($F^2 > 2\sigma(F^2)$)	0.0805; 0.0825	0.0920; 0.0945
$\Delta\rho_{max}$; $\Delta\rho_{min}$ (e·Å^{-3})	0.570; −0.486	0.869; −0.466

[a] Estimated standard deviations are given in parentheses.

Table 2. Atomic coordinates, isotropic displacement parameters [Å^2], and occupation of crystallographic positions of $MgH_4P_6N_{12}$.[a]

Atom	Wyck.	x	y	z	U_{eq} [Å^2]
Mg1	4*a*	0	0	0	0.0094(3)
P1	16*g*	0.33547(6)	−0.00404(10)	0.08754(2)	0.00648(17)
P2	8*f*	0.0000	0.40462(15)	0.21131(3)	0.00779(19)
N1	16*g*	0.1523(2)	0.4808(4)	0.16633(8)	0.0085(3)
N2	16*g*	0.3154(2)	0.3150(4)	0.06601(8)	0.0079(3)
N3	8*f*	0	0.0778(5)	0.22543(12)	0.0117(5)
N4	8*f*	0	0.3694(5)	0.06269(11)	0.0074(4)
H1	16*g*	0.241(3)	0.492(8)	0.1862(18)	0.048(11)

[a] Estimated standard deviations are given in parentheses.

Table 3. Atomic coordinates, isotropic displacement parameters [Å^2], and occupation of crystallographic positions of $CaH_4P_6N_{12}$.[a]

Atom	Wyck.	x	y	z	U_{eq} [Å^2]
Ca1	4*a*	0	0	0	0.0064(3)
P1	16*g*	0.33608(9)	0.00519(15)	0.09419(4)	0.0073(3)
P2	8*f*	0	0.4215(2)	0.21316(5)	0.0100(3)
N1	16*g*	0.1505(3)	0.4948(5)	0.17004(12)	0.0094(5)
N2	16*g*	0.3052(3)	0.3158(5)	0.07270(12)	0.0103(6)
N3	8*f*	0.0000	0.0986(8)	0.22686(18)	0.0148(8)
N4	8*f*	0.0000	0.4003(7)	0.06900(17)	0.0100(7)
H1	16*g*	0.225(7)	0.522(15)	0.197(3)	0.10(3)

[a] Estimated standard deviations are given in parentheses.

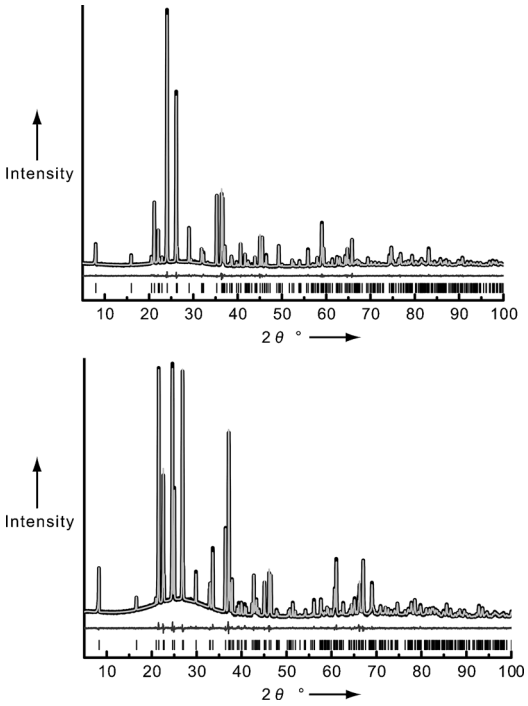

Figure 2. Rietveld refinements of $MH_4P_6N_{12}$, M = Mg (top), Ca (bottom); observed (black line) and calculated (light-gray line) X-ray powder diffraction patterns, positions of Bragg reflections (vertical black bars), and difference profile (dark-gray line).

from single-crystal data and confirmed the presence of a crystalline single-phase product (see Figure 2). The crystallographic data as well as atomic parameters of the Rietveld refinement of $MH_4P_6N_{12}$ are summarized in Tables S1, S2, and S3.

The chemical compositions of the title compounds were determined by energy-dispersive X-ray (EDX) spectroscopy. No elements other than Mg/Ca, P, and N were detected. Trace amounts of oxygen were most probably attributable to surface hydrolysis of the sample. The atomic ratio (Ca/Mg):P:N was in good agreement with the predicted composition of the products. In calculating the chemical composition, it was kept in mind that hydrogen atoms cannot be detected by EDX. The results of the EDX analysis are summarized in Tables S4 and S5 (Supporting Information).

The FTIR spectra of $MgH_4P_6N_{12}$ and $CaH_4P_6N_{12}$ are very similar, reflecting the structural similarity of these compounds (see Figure S1). Both spectra feature a significantly wide multiple absorption band between 2538 and 3250 cm^{-1}. This can be attributed to the N–H valence modes of the NH groups of the layers. Additionally, absorption bands between 400 and 1500 cm^{-1} can be observed, which are characteristic of nitridophosphates. The latter can be assigned to symmetric and asymmetric P-N-P stretching modes.

Solid-state NMR study

The aim of the solid-state NMR study was to corroborate the models obtained from single-crystal X-ray diffraction analysis, mainly with respect to the H atoms, since these possess a low scattering power in diffraction experiments. In the following, we identify the expected ^{31}P and ^{1}H NMR signals, quantify the latter, and finally demonstrate ^{31}P-^{1}H spatial proximity.

The unit cells of the title compounds both feature two P sites with an atomic ratio P1:P2 = 2:1 (see Tables 2 and 3). The ^{31}P MAS NMR spectra of $MgH_4P_6N_{12}$ and $CaH_4P_6N_{12}$ are consistent with this model, showing two main peaks with the expected area ratio (see Figure S2). These two signals correlate with one another, showing double-quantum filtered peaks (see Figures 3 and S3), and thus confirm that the peaks assigned to P1 and P2 arise from the same phase.

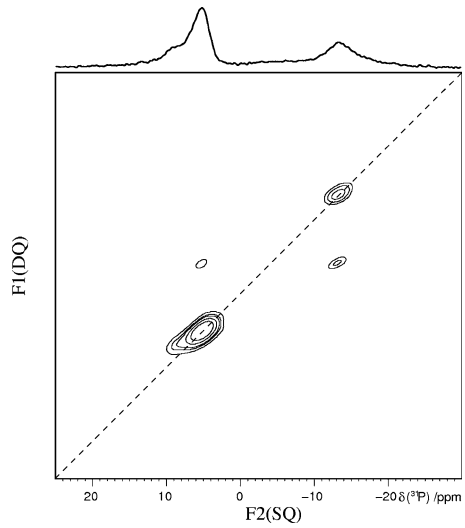

Figure 3. ^{31}P–^{31}P 2D double-quantum (DQ) single-quantum (SQ) correlation MAS NMR spectrum of $MgH_4P_6N_{12}$ obtained at a sample spinning frequency of 20 kHz. The dashed diagonal line denotes the peak position of isochronous spins (autocorrelation peaks).

Each of the solid-state ^{1}H NMR spectra (see Figure 4) features one peak attributable to the respective title compounds ($\delta \approx 6.5$ ppm). The other peak is assigned to an unknown side phase, which may contain NH_4^+ from the mineralizer NH_4Cl ($\delta = 7.3$ ppm). For comparison, the solid-state ^{1}H NMR spectrum of pure NH_4Cl is shown in Figure S4 (Supporting Information). Moreover, the hydrogen contents were quantified as 3.8 ± 0.4 and 3.9 ± 0.4 hydrogen atoms per chemical formula

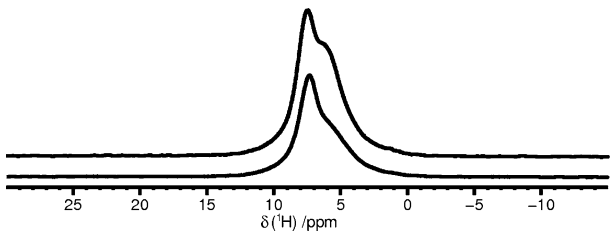

Figure 4. ^{1}H MAS NMR spectra of $MgH_4P_6N_{12}$ (bottom) and $CaH_4P_6N_{12}$ (top), measured at a sample spinning frequency of 40 kHz. The sharp peak at around 7.4 ppm in each spectrum is due to NH_4Cl, which was used as a mineralizer, while the other peak at around 6 ppm is assigned to the respective title compounds.

unit of the magnesium and calcium compounds, respectively. These numbers support the models obtained from single-crystal structure solution and FTIR spectroscopy, confirming the chemical compositions $MgH_4P_6N_{12}$ and $CaH_4P_6N_{12}$.

Finally, the question remains as to whether the P atoms belong to the same phase as the quantified hydrogen atoms. The proximity of P1 and P2 to hydrogen was confirmed by $^{31}P\{^1H\}$ heteronuclear correlation NMR (see Figures 5 and 6), with each spectrum showing two ^{31}P-^1H correlation peaks.

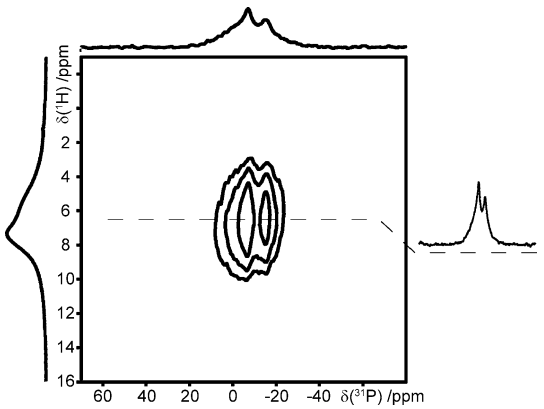

Figure 5. $^{31}P\{^1H\}$ heteronuclear correlation spectrum of $CaH_4P_6N_{12}$ measured at a sample spinning frequency of 20 kHz. Correlation peaks are shown as a contour plot.

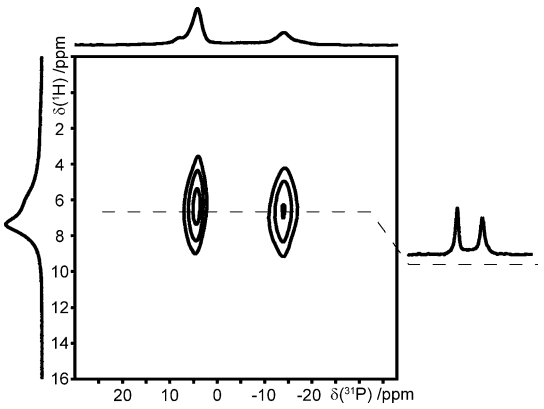

Figure 6. $^{31}P\{^1H\}$ heteronuclear correlation spectrum of $MgH_4P_6N_{12}$ measured at a sample spinning frequency of 20 kHz. Correlation peaks are shown as a contour plot.

Structure description

The crystal structure of $MH_4P_6N_{12}$ (M = Mg, Ca) consists of a layered network of all-side vertex-sharing Q^4-type PN_4 tetrahedra, leading to a degree of condensation $\kappa = n(P):n(N) = 0.5$ for the $_\infty{}^3[P^{[4]}{}_6N^{[2]}{}_8(NH)^{[2]}{}_4]^{6-}$ substructure (see Figure 7). The PN_4 tetrahedra form double layers, which are oriented parallel to the *ab* plane. These layers are separated by Mg and Ca, respectively.

The topology of these layers is represented by the point symbol $\{3.6^5\}$ (determined by TOPOS software[25]) and has not

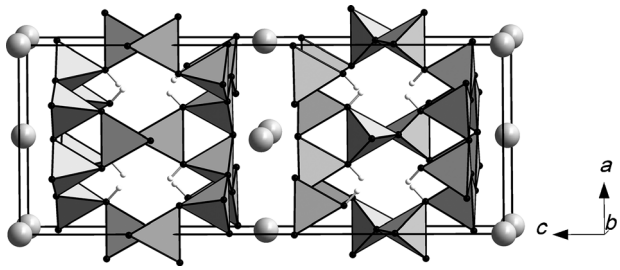

Figure 7. Crystal structure of $MH_4P_6N_{12}$ (M = Mg, Ca) viewed approximately along [010]. Light-gray alkaline-earth atoms Mg or Ca; dark-gray PN_4 tetrahedra, white H atoms.

been found in any other known compound so far. Condensation of PN_4 tetrahedra results in *dreier* and *sechser* rings, according to the nomenclature introduced by Liebau.[26] These form rhombic channels, in which H atoms are covalently bound to N1 atoms (see Figure 7).

Each double layer can be subdivided into two opposing planar *sechser* ring single layers, which are mutually staggered (see Figure 8b). These single layers are interconnected by *zweier* zigzag single chains parallel to the *b*-axis (see Figure 8a). According to the nomenclature introduced by

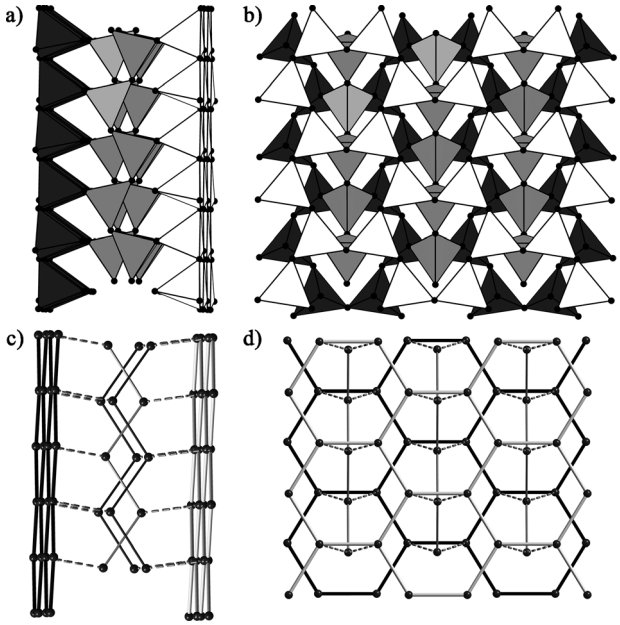

Figure 8. A *sechser* ring double layer in $MH_4P_6N_{12}$, viewed along [100] (a) and [001] (b), with the respective topological representations (c, d). White and black PN_4 tetrahedra belong to different *sechser* ring single layers, dark-gray PN_4 tetrahedra represent *zweier* single chains. Each connecting line in the topological representation represents a P-N-P bond. The dotted lines represent P-N-P bonds between a zigzag chain and a *sechser* ring layer.

Liebau,[26] the terms "*zweier*", "*dreier*", and "*sechser*" derive from the German words "zwei", "drei", and "sechs", meaning two, three, and six, respectively. Accordingly, a *zweier* single chain includes two PN_4 tetrahedra within one repeating unit of the linear part of the chain. Topological representation of the *sechser* ring double layers illustrates the arrangement of these

condensed rings in a honeycomb-like pattern (see Figure 8c, d).

The P–N bond lengths and P-N-P angles in both samples vary in similar ranges [Mg: 1.586(3)–1.684(2) Å, 119.7(2)–132.6(2)°; Ca: 1.587(4)–1.685(3) Å, 123.6(2)–134.0(3)°]. This can be rationalized by the fact that the layers contain no Mg or Ca atoms and thus are not affected by their size. The P–N bond lengths and P-N-P angles correspond to those usually observed in other imidonitridophosphates.[22,23] As expected, the P–(NH)[2] bond lengths [Mg: 1.684(2) Å; Ca: 1.685(3) Å] are significantly longer than the P–N[2] bond lengths [Mg: 1.586(3)–1.616(2) Å; Ca: 1.587(4)–1.617(3) Å], in good agreement with the localization of the H atoms in the structure model. Detailed information on the bond lengths and angles is given in Table 4.

Table 4. Bond lengths [Å] and bond angles [°] in the crystal structures of $MH_4P_6N_{12}$, M = Mg, Ca.[a]

	Mg	Ca		Mg	Ca
P1–N2	1.613(2)	1.604(3)	P2–N1	1.647(2)	1.652(3)
P1–N4	1.610(1)	1.605(2)	P1-N1-P2	129.6(1)	129.6(2)
P1–N2	1.616(2)	1.617(3)	P1-N2-P1	121.3(1)	125.6(2)
P1–N1	1.684(2)	1.685(3)	P2-N3-P2	132.6(2)	134.0(3)
P2–N3	1.586(3)	1.587(4)	P1-N4-P1	119.7(2)	123.6(2)
P2–N3	1.606(3)	1.611(4)			

[a] Estimated standard deviations are given in parentheses.

A similar structural motif of double layers can be found in $LiSrGaN_2$.[23] However, the *sechser* ring single layers in the structure of this compound are not planar and are interconnected by edge-sharing pairs of GaN_4 tetrahedra, rather than *zweier* single chains. Furthermore, the structural motif of the almost planar *sechser* ring single layers can be found in layered silica compounds, such as muscovite and pyrophyllite, in which two opposing layers $_\infty{}^2[Si_2O_5]^{2-}$ are interconnected by the edge-sharing Al-centered octahedral units of oxyhydroxides.[26–29]

The metal atoms occupy only one crystallographic site in the crystal structure. They are coordinated by six N atoms at distances of 2.228(2)–2.283(2) Å (M = Mg) and 2.492(4)–2.501(4) Å (M = Ca), respectively, in a slightly distorted octahedral arrangement (see Figure 9). These M–N distances are in good agreement with those in other known Mg (2.056–2.248 Å, CN(Mg) = 6)[30–33] and Ca compounds (2.419–2.598 Å, CN(Ca) = 6),[34,35] as well as with the sums of the ionic radii.[36] The MN_6 octahedra are not interconnected with each other (see Figure 9c). As only the N2 and N4 atoms belong to the coordination spheres of the respective metal atoms, it is reasonable that the P1-N2-P1 and P1-N4-P1 bond angles are larger in $CaH_4P_6N_{12}$ than in $MgH_4P_6N_{12}$, whereas the P1-N1-P2 and P2-N3-P2 bond angles remain almost identical.

Conclusion

$MH_4P_6N_{12}$ (M = Mg, Ca) represent new imidonitridophosphates with an unprecedented layered structure type. By adding catalytic amounts of NH_4Cl, single crystals of the title compounds could be obtained and isolated. The hydrogen contents of the samples have been determined by quantitative solid-state ^{1}H NMR and support the models obtained from single-crystal structure solution. The layered structures of these compounds consist of condensed *sechser* rings arranged in a honeycomb-like pattern, alternating with metal ion layers. Both compounds are air- and moisture-stable. According to their structural features and material properties, $MH_4P_6N_{12}$ (M = Mg, Ca) appear to be promising candidates for liquid exfoliation of the single layers in order to obtain two-dimensional single nanomaterials. Additionally, the unusual layered structure of these compounds may lead to their use as gas absorbers or as ionic conductors. However, further investigations on the ion-exchange or intercalation properties of these compounds need to be carried out. Furthermore, considering the sandwich-type structure of the obtained materials, the synthesis of isotypic compounds by exchange of the alkaline-earth cations may lead to interesting new properties. Finally, it should be noted that the high-pressure/high-temperature synthesis proved to be a very promising route for the synthesis of new nitridophosphates with interesting structural properties.

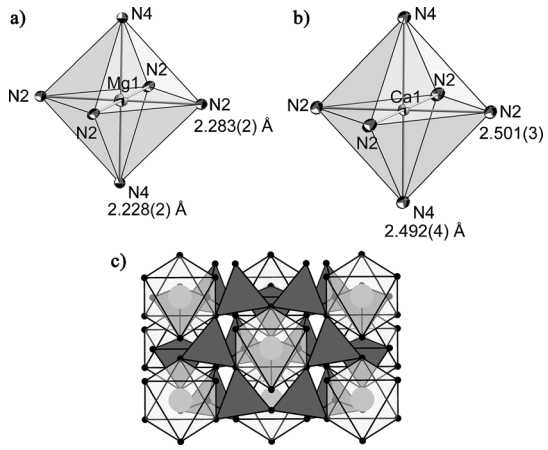

Figure 9. Coordination polyhedra and corresponding bond lengths [Å] of the Ca1 position in $CaH_4P_6N_{12}$ (a) and the Mg1 position in $MgH_4P_6N_{12}$ (b); ellipsoids are drawn with a probability factor of 70%; the arrangement of the MN_6 (M = Mg, Ca) octahedra in the *sechser* ring layers (c).

Experimental Section

Preparations of starting materials

Ca_3N_2 and Mg_3N_2 were synthesized by heating Ca (dendritic pieces, 99.99% trace metal basis, Sigma–Aldrich) or Mg (chips, 99%, *reinst*, Grüssing), respectively, in a ceramic corundum boat at 950 °C (8 h) in a continuous flow of dried N_2. Ca_3N_2 was obtained as a dark-violet solid, and Mg_3N_2 was obtained as a dark-yellow solid. Detailed information is available in the literature.[37] The phase purities of the respective products were confirmed by powder X-ray diffraction analysis and FTIR spectroscopy.

P_3N_5 and amorphous HPN_2 were synthesized by heating $(PNCl_2)_3$ (Merck, p.s.) in a ceramic corundum boat at 100 °C (10 h), 130 °C (5 h), 190 °C (3 h), and 300 °C (4 h) in a continuous flow of dried

NH_3 (Air Liquide, 5.0), followed by vacuum heat treatment of the mixture at 600 °C (2 h) to obtain P_3N_5 or at 450 °C (2 h) to obtain amorphous HPN_2. In the case of P_3N_5, the mixture was additionally heated at 950 °C (2 h). This step was essential for complete condensation of the product. Detailed information is available in the literature.[38–41] The phase purities of the respective products were confirmed by powder X-ray diffraction analysis and FTIR spectroscopy.

Synthesis

$MH_4P_6N_{12}$ (M = Mg, Ca) were synthesized from stoichiometric amounts of the respective alkaline-earth metal nitrides and amorphous HPN_2 and P_3N_5 using a Walker-type multi-anvil apparatus.[6] A catalytic amount of NH_4Cl was used as a mineralizer. Because of the high air-sensitivity of Mg_3N_2 and Ca_3N_2, all manipulations were carried out under exclusion of oxygen and moisture in an argon-filled glove box (Unilab, MBraun, Garching, $O_2 < 1$ ppm, $H_2O <$ 0.1 ppm). The respective starting mixture was thoroughly ground and tightly packed into a cylindrical capsule of hexagonal boron nitride (Henze, Kempten). The filled capsule was sealed with a hexagonal boron nitride cap and placed in the center of a Cr_2O_3-doped MgO octahedron (edge length 18 mm, Ceramic Substrates & Components Ltd., Isle of Wight, U.K.). The MgO octahedron was equipped with a ZrO_2 tube (Cesima Ceramics, Wust-Fischbach, Germany), which served as a thermal insulator. Furthermore, two graphite tubes (one long tube and one short tube) were used as electrical resistance furnaces. In order to ensure that the short graphite tube was positioned in the center of the long tube, two MgO spacers (one on each side) were used. Finally, a Mo plate was placed on each side of the ZrO_2 tube in order to achieve electrical contact between the graphite tubes and the anvils of the multi-anvil press. The MgO octahedron was then placed in the center of an assembly of eight truncated tungsten carbide cubes (truncation edge lengths 11 mm, Hawedia, Marklkofen, Germany), which were separated with pyrophyllite gaskets. Detailed information on the construction of the described multi-anvil assembly can be found in the literature.[19] The sample was compressed to 8 GPa at room temperature. It was then heated to 1000 °C over a period of 60 min, and the temperature was held at this level for 120 min. Subsequently, the sample was cooled to room temperature over a period of 60 min. After slow decompression (10 h), both products were recovered as colorless crystalline solids, which were not sensitive to air or moisture. NH_4Cl was removed from the products by washing with water and ethanol. However, for the solid-state NMR experiments, the washing step was omitted.

Single-crystal X-ray diffraction analysis

Single-crystal X-ray diffraction data were collected on a Nonius Kappa CCD diffractometer ($Mo_{K\alpha}$ radiation, graphite monochromator, Bruker, Karlsruhe). A semi-empirical absorption correction was applied using the program XPREP.[42] The crystal structures were solved by direct methods using SHELXS,[42] and refined by full-matrix least-squares methods using SHELXL.[43] Further details of the crystal structure determinations can be obtained from the Fachinformationszentrum Karlsruhe, 76344 Eggenstein-Leopoldshafen, Germany (Fax: +49–7247–808–666; e-mail: crysdata@fiz-karlsruhe.de) on quoting the depository numbers CSD-427952 ($MgH_4P_6N_{12}$) and CSD-427953 ($CaH_4P_6N_{12}$).

Powder X-ray diffraction analysis

Powder X-ray diffraction data for both compounds were collected on a STOE StadiP powder diffractometer ($Cu_{K\alpha1}$ radiation, Ge(111) monochromator, MYTHEN 1 K Si strip detector) in parafocusing Debye–Scherer geometry. Rietveld refinements were carried out using the TOPAS Academic 4.1 package.[44] The preferred orientation of the crystallites was described using a fourth-order spherical harmonic. Peak shapes were modeled by the fundamental parameters approach (direct convolution of source emission profiles, axial instrument contributions, and crystallite size and microstrain effects).

Solid-state NMR spectroscopy

For all measurements, the ^1H resonance of 1% $Si(CH_3)_4$ in $CDCl_3$ served as an external secondary reference, using the Ξ value for ^{31}P relative to 85% H_3PO_4 as reported by the IUPAC.[45] Solid-state NMR spectra were measured on a Bruker Avance III spectrometer with an 11.7 T magnet, operating at a ^1H frequency of 500.25 MHz, equipped with commercial 1.3 mm and 2.5 mm double-resonance MAS probes. ^{31}P–^{31}P 2D double-quantum (DQ) single-quantum (SQ) correlation MAS NMR spectra were obtained at a sample spinning frequency of 20 kHz with a transient-adapted POSTC7 sequence.[46,47] The conversion period was set at 1.2 ms. Rotor-synchronized data sampling of the indirect dimension accumulated 16 transients per FID. Proton decoupling was implemented by CW decoupling with a nutation frequency of 110 kHz. Repetition delays were set at 60 s and 42 s for $MgH_4P_6N_{12}$ and $CaH_4P_6N_{12}$, respectively. $^{31}P\{^1H\}$ heteronuclear correlation MAS NMR spectra were obtained through a 2D correlation experiment based on the PRESTO II pulse sequence[48] as described in the literature.[49] Here, proton decoupling was implemented by TPPM decoupling[50] with a nutation frequency of 115 kHz. The ^1H nutation frequency for the $R18_2^5$ recoupling sequence was 90 kHz for the R-elements, which consisted of simple π-pulses. All other hard pulses applied in both channels were implemented with a nutation frequency of 100 kHz. Both experiments were performed at a sample spinning frequency of 20 kHz with a repetition delay of 1.5 s. The numbers of accumulated transients per FID were 256 and 512 for $MgH_4P_6N_{12}$ and $CaH_4P_6N_{12}$, respectively.

FTIR spectroscopy

The FTIR spectra of $MH_4P_6N_{12}$ (M = Mg, Ca) were measured using the KBr pellet method on a Spectrum BX II spectrometer (Perkin-Elmer, Waltham MA, USA).

Scanning electron microscopy and energy-dispersive X-ray spectroscopy

SEM imaging and EDX analysis were performed using a JEOL JSM-6500 F field-emission scanning electron microscope (SEM), equipped with a Si/Li EDX detector 7418 (Oxford Instruments). In order to impart electrical conductivity to the sample surfaces, they were coated with carbon using an electron beam evaporator (BAL-TEC MED 020, Bal Tec AG).

Acknowledgements

We thank Dr. Peter Mayer for collecting single-crystal X-ray data and Christian Minke for EDX measurements. Furthermore, we gratefully acknowledge financial support from the Fonds

der Chemischen Industrie (FCI) and the Deutsche Forschungsgemeinschaft (DFG).

Keywords: high-pressure chemistry · high-temperature chemistry · imidonitridophosphates · layered compounds · solid-state structures

[1] M. Zeuner, S. Pagano, W. Schnick, *Angew. Chem. Int. Ed.* **2011**, *50*, 7754; *Angew. Chem.* **2011**, *123*, 7898.
[2] H. Huppertz, W. Schnick, *Z. Anorg. Allg. Chem.* **1997**, *623*, 212.
[3] F. Karau, W. Schnick, *Angew. Chem. Int. Ed.* **2006**, *45*, 4505; *Angew. Chem.* **2006**, *118*, 4617.
[4] D. Baumann, S. J. Sedlmaier, W. Schnick, *Angew. Chem. Int. Ed.* **2012**, *51*, 4707; *Angew. Chem.* **2012**, *124*, 4785.
[5] S. Correll, O. Oeckler, N. Stock, W. Schnick, *Angew. Chem. Int. Ed.* **2003**, *42*, 3549; *Angew. Chem.* **2003**, *115*, 3674.
[6] S. Correll, N. Stock, O. Oeckler, J. Senker, T. Nilges, W. Schnick, *Z. Anorg. Allg. Chem.* **2004**, *630*, 2205.
[7] S. J. Sedlmaier, M. Döblinger, O. Oeckler, J. Weber, J. Schmedt auf der Günne, W. Schnick, *J. Am. Chem. Soc.* **2011**, *133*, 12069.
[8] M. S. Choudhary, J. K. Fink, K. Lederer, H. A. Krässig, *J. Appl. Polym. Sci.* **1987**, *34*, 863.
[9] a) Y. H. Jeong, J. H. Lee, Y. T. Hong, *Appl. Phys. Lett.* **1990**, *57*, 2680; b) Y. H. Jeong, G. T. Kim, K. I. Kim, U. J. Jeong, *J. Appl. Phys.* **1991**, *69*, 6699; c) Y. Hirota, T. Hisaki, O. Mikami, *Electron. Lett.* **1985**, *21*, 690.
[10] J. A. Graves, U.S. Patent 3475072, **1969**.
[11] T. Grande, J. R. Holloway, P. F. McMillan, C. A. Angell, *Nature* **1994**, *369*, 43.
[12] T. Grande, S. Jacob, J. R. Holloway, P. F. McMillan, C. A. Angell, *J. Non-Cryst. Solids* **1995**, *184*, 151.
[13] S. V. Levchik, G. F. Levchik, A. I. Balabanovich, E. D. Weil, M. Klatt, *Angew. Makromol. Chem.* **1999**, *264*, 48.
[14] E. D. Weil, N. G. Patel, *Fire Mater.* **1994**, *18*, 1.
[15] M. Pouchard, *Nature* **2006**, *442*, 878.
[16] W. Schnick, J. Lücke, *Solid State Ionics* **1990**, *38*, 271.
[17] W. Schnick, J. Lücke, *Z. Anorg. Allg. Chem.* **1992**, *610*, 121.
[18] A. Marchuk, F. J. Pucher, F. W. Karau, W. Schnick, *Angew. Chem. Int. Ed.* **2014**, *53*, 2469; *Angew. Chem.* **2014**, *126*, 2501.
[19] S. Horstmann, E. Irran, W. Schnick, *Z. Anorg. Allg. Chem.* **1998**, *624*, 221.
[20] D. Baumann, W. Schnick, *Inorg. Chem.* **2014**, *53*, 7977.
[21] D. Baumann, W. Schnick, *Angew. Chem. Int. Ed.* **2014**, *53*, 14490; *Angew. Chem.* **2014**, *126*, 14718.
[22] H. Jacobs, S. Pollok, F. Golinski, *Z. Allg. Anorg. Chem.* **1994**, *620*, 1213.
[23] F. Golinski, H. Jacobs, *Z. Allg. Anorg. Chem.* **1995**, *621*, 29.
[24] a) N. Kawai, S. Endo, *Rev. Sci. Instrum.* **1970**, *41*, 1178; b) D. Walker, M. A. Carpenter, C. M. Hitch, *Am. Mineral.* **1990**, *75*, 1020; c) D. Walker, *Am. Mineral.* **1991**, *76*, 1092; d) D. C. Rubie, *Phase Transitions* **1999**, *68*, 431; e) H. Huppertz, *Z. Kristallogr.* **2004**, *219*, 330.
[25] V. A. Blatov, A. P. Shevchenko, D. M. Proserpio, *Cryst. Growth Des.* **2014**, *14*, 3576.
[26] F. Liebau, *Structural Chemistry of Silicates*, Springer, Berlin, **1985**.
[27] D. G. Park, Z. A. Gal, F. J. DiSalvo, *J. Alloys Compd.* **2003**, *353*, 107.
[28] R. Wardle, G. W. Brindley, *Am. Mineral.* **1972**, *57*, 732.
[29] E. W. Radoslovich, *Acta. Crystallogr.* **1960**, *13*, 919.
[30] F. Karau, W. Schnick, *Z. Allg. Anorg. Chem.* **2006**, *632*, 49.
[31] B. Jürgens, E. Irran, W. Schnick, *J. Solid State Chem.* **2001**, *157*, 241.
[32] H. Hiraguchi, H. Hashizume, S. Sasaki, S. Nakano, O. Fukunaga, *Acta Crystallogr. Sect. B* **1993**, *49*, 478.
[33] A. Marchuk, L. Neudert, O. Oeckler, W. Schnick, *Eur. J. Inorg. Chem.* **2014**, 3427.
[34] S. J. Clarke, F. J. DiSalvo, *Inorg. Chem.* **1997**, *36*, 1143.
[35] M. S. Bailey, F. J. DiSalvo, *J. Alloys Compd.* **2006**, *417*, 50.
[36] W. H. Baur, *Crystallogr. Rev.* **1987**, *1*, 59.
[37] O. Reckeweg, F. J. DiSalvo, *Z. Anorg Allg. Chem.* **2001**, *627*, 371.
[38] F. W. Karau, *Dissertation*, Ludwig-Maximilians-Universität München (Germany) **2007**.
[39] J. Lücke, *Dissertation*, Rheinische Friedrich-Wilhelms-Universität Bonn (Germany) **1994**.
[40] W. Schnick, J. Lücke, F. Krumeich, *Chem. Mater.* **1996**, *8*, 281.
[41] S. Horstmann, E. Irran, W. Schnick, *Angew. Chem. Int. Ed. Engl.* **1997**, *36*, 1873; *Angew. Chem.* **1997**, *109*, 1938.
[42] G. M. Sheldrick, XPREP, Data Preparation & Reciprocal Space Exploration, **1996**, v6.12, Siemens Analytical X-ray Instruments.
[43] G. M. Sheldrick, *Acta Crystallogr. Sect. A* **2008**, *64*, 112.
[44] A. A. Coelho, *TOPAS-Academic*, Version 4.1, Coelho Software, Brisbane (Australia), **2007**.
[45] R. K. Harris, E. D. Becker, S. M. Cabral de Menezes, P. Granger, R. E. Hoffman, K. W. Zilm, *Pure Appl. Chem.* **2008**, *80*, 59.
[46] M. Hohwy, H. J. Jakobsen, M. Edén, M. H. Levitt, N. C. Nielsen, *J. Chem. Phys.* **1998**, *108*, 2686.
[47] J. Weber, M. Seemann, J. Schmedt auf der Günne, *Solid State Nucl. Magn. Reson.* **2012**, *43–44*, 42.
[48] X. Zhao, W. Hoffbauer, J. Schmedt auf der Günne, M. H. Levitt, *Solid State Nucl. Magn. Reson.* **2004**, *26*, 57.
[49] Y. S. Avadhut, J. Weber, E. Hammarberg, C. Feldmann, J. Schmedt auf der Günne, *Phys. Chem. Chem. Phys.* **2012**, *14*, 11610.
[50] A. E. Bennett, C. M. Rienstra, M. Auger, K. V. Lakshmi, R. G. Griffin, *J. Chem. Phys.* **1995**, *103*, 6951.

Received: November 26, 2014
Published online on ■■ ■■, 0000

FULL PAPER

Layered Imidonitridophosphates

A. Marchuk, V. R. Celinski, J. Schmedt auf der Günne, W. Schnick**

■■ – ■■

$MH_4P_6N_{12}$ (M = Mg, Ca): New Imidonitridophosphates with an Unprecedented Layered Network Structure Type

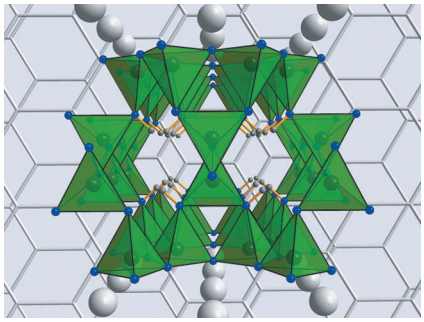

Unprecedented layered structure: New imidonitridophosphates $MH_4P_6N_{12}$ (M = Mg, Ca) have been synthesized by high-pressure/high-temperature reactions at 8 GPa and 1000 °C. Their crystal structures have been determined by single-crystal X-ray diffraction analyses and confirmed by Rietveld refinement, which reveal an unprecedented layered structure type (see graphic). The hydrogen contents of the samples have been quantified by solid-state NMR spectroscopy.